Bioorganic & Medicinal Chemistry 20 (2012) 2221–2226

Contents lists available at SciVerse ScienceDirect

Bioorganic & Medicinal Chemistry

journal homepage: www.elsevier.com/locate/bmc

Synthesis and evaluation of fluorobenzoylated di- and tripeptides as inhibitors of cyclooxygenase-2 (COX-2)

Sai Kiran Sharma [a,b], Baker Jawabrah Al-Hourani [a], Melinda Wuest [a], Jonathan Y. Mane [a], Jack Tuszynski [a], Vickie Baracos [a], Mavanur Suresh [b], Frank Wuest [a,b,*]

[a] Department of Oncology, University of Alberta, Edmonton, Canada
[b] Faculty of Pharmacy and Pharmaceutical Sciences, University of Alberta, Edmonton, Canada

ARTICLE INFO

Article history:
Received 15 December 2011
Revised 28 January 2012
Accepted 7 February 2012
Available online 15 February 2012

Keywords:
Cyclooxygenase
COX-2 inhibitors
Peptides
Molecular probes

ABSTRACT

A series of fluorobenzoylated di- and tripeptides as potential leads for the development of molecular probes for imaging of COX-2 expression was prepared according to standard Fmoc-based solid-phase peptide synthesis. All peptides were assessed for their COX-2 inhibitory potency and selectivity profile in a fluorescence-based COX binding assay. Within the series of 15 peptides tested, cysteine-containing peptides numbered **7**, **8**, **11** and **12**, respectively, were the most potent COX-2 inhibitors possessing IC_{50} values ranging from 5 to 85 μM. Fluorobenzoylated tripeptides **7** and **8** displayed some COX-2 selectivity (COX-2 selectivity index 2.1 and 1.6), whereas fluorobenzoylated dipeptides **11** and **12** were shown not to be COX-2 selective. Fluorbenzoylated tripeptide FB-Phe-Cys-Ser-OH was further used in molecular modeling docking studies to determine the binding mode within the active site of the COX-2 enzyme.

1. Introduction

Cyclooxygenases (COXs) catalyze the first steps of the complex conversion of arachidonic acid to prostaglandins and thromboxanes, which mediate as locally active messenger molecules many physiological events and pathogenetic pathways.[1–3] Cycloogygenases exist in two distinct isoforms, a constitutive form (COX-1) and an inducible form (COX-2). The COX-1 enzyme is expressed in resting cells of most tissues, functions as a housekeeping enzyme, and is responsible for maintaining homeostasis (gastric and renal integrity) and normal production of prostaglandins. COX-2 is predominantly found in brain, kidney and endothelial cells, but is virtually absent in most other tissues. However, COX-2 expression is significantly upregulated as part of various acute and chronic inflammatory conditions, and in neoplastic tissues.

COX-1 and COX-2 share arachidonic acid as their natural substrate. They both catalyze in a cyclooxygenase reaction the conversion of arachidonic acid into prostaglandin PGG_2 which is further converted in a peroxidase reaction into PGH_2 by a two electron reduction. The X-ray crystal structures of both enzymes suggest that the tertiary conformations of these proteins are very similar. The amino acids which constitute the substrate binding pocket and catalytic site are nearly identical in both enzymes.[4–6] The only difference is in amino acid residues at positions 434 and 523 in COX-1 and COX-2, respectively, which is isoleucine in the case of COX-1 and valine in COX-2. The structural similarities of COX-1 and COX-2 enzyme have made the development of selective inhibitors for COX-2 versus COX-1 a special challenge. Moreover, recent studies have demonstrated that some selective COX-2 inhibitory drugs are associated with harmful cardiovascular events like high blood pressure and myocardial infarction.[7,8] This led to the withdrawal of rofecoxib and valdecoxib from the market and has constantly stimulated the search for new classes of selective COX-2 inhibitors including compounds containing NO-donors.

Since the discovery of the COX-2 enzyme in the early 1990s, numerous COX-2 selective inhibitors have been proposed. Figure 1 displays a selection of prominent selective COX-2 inhibitors.

A common structural feature of these selective COX-2 inhibitors is the presence of two vicinal aryl rings attached to a central five or six-membered heterocyclic or carbocyclic motif. Typical examples of selective COX-2 inhibitors like celecoxib, rofecoxib, valdecoxib, etoricoxib, and SC57666 demonstrate that a broad variety of five- or six-membered carbo- and heterocycles are acceptable for binding to the cyclooxygenase active site.

Recent reviews on the current status of COX-2 inhibitors further confirm the flexibility of the carbocyclic/heterocyclic core motif for COX-2 binding.[9–12] However, recently various small peptides were described as an alternative class of potent and selective COX-2 inhibitors.[13–16] Based on the COX-1 and COX-2 X-ray crystal structures with known inhibitors and computer-aided rational drug design, a library of several tripeptides was prepared and tested using surface plasmon resonance and other biochemical methods in order to elucidate in vitro COX-2 potency and selectivity. Various

* Corresponding author. Tel.: +1 780 989 8150; fax: +1 780 432 8483.
E-mail address: wuest@ualberta.ca (F. Wuest).

0968-0896/$ - see front matter © 2012 Elsevier Ltd. All rights reserved.
doi:10.1016/j.bmc.2012.02.021

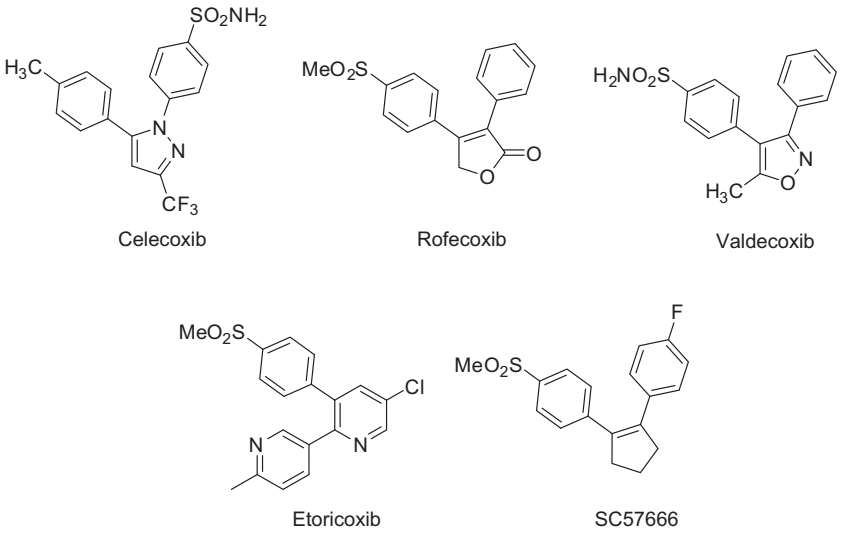

Figure 1. Chemical structures of selective COX-2 inhibitors.

tripeptide inhibitors showed remarkably high affinity towards COX-2 in subnanomolar range while retaining high selectivity. These data suggest that small peptide inhibitors may serve as suitable compounds for the design of a novel class of highly potent and selective COX-2 inhibitors in addition to the known class of prominent small molecule inhibitors as depicted in Figure 1.

Our research group has long-standing interest in the development of molecular probes for imaging COX-2 expression in vivo.[17,18] Over the last decade, all attempts to develop molecular probes for imaging functional COX-2 expression in vivo were based on small molecule inhibitors. Most of this work was devoted to the development of radiotracers for COX-2 imaging by means of positron emission tomography (PET) as the currently most sophisticated functional molecular imaging methodology. As a result, several ^{18}F- and ^{11}C-labeled analogues of prominent COX-2 inhibitors DuP-697, celecoxib, rofecoxib, valdecoxib, and other compounds containing a heterocycle core structure have been synthesized and, in some cases, radiopharmacologically evaluated in vivo as potential PET radiotracers for imaging of COX-2. However, all radiolabeled COX-2 inhibitors tested showed unfavorable radiopharmacological profiles for molecular imaging of COX-2 expression in vivo, mainly due to high nonspecific binding and high metabolic instability.[17–21]

Based on previous reports describing tripeptides as highly potent and selective COX-2 inhibitors, this work describes the design, synthesis and evaluation of a series of fluorobenzoylated di- and tripeptides as novel selective COX-2 inhibitors as potential lead compounds towards the development of peptide-based molecular probes for molecular imaging COX-2 expression in vivo. Peptides can be labeled with short-lived positron emitter fluorine-18 ($t_{1/2}$ = 108.9 min, ^{18}F) using various techniques.[22] Conjugation of the bifunctional labeling agent 4-succinimidyl-[^{18}F]fluorobenzoate ([^{18}F]SFB) to the N-terminal end of the peptide backbone is among the most commonly employed techniques.[23–26] All peptides were tested for their COX-2 inhibitory potency and selectivity in an in vitro COX binding assay. Experimental assays were followed and supported by molecular modeling docking experiments that used the most potent and selective fluorobenzoylated tripeptide.

2. Results and discussion

The COX active site in the enzyme interior is connected to the membrane by a long non-polar channel, and the active site of COX contains mainly hydrophobic amino acid residues. Most of the known selective COX-2 inhibitors (Fig. 1) contain sulfur as exemplified by the commonly found sulfonamide or methylsulfone moiety as in celecoxib (sulfonamide) or rofecoxib (methylsulfone). Based on this information, various tripeptide sequences containing an aromatic hydrophobic amino acid (e.g. tryptophan, tyrosine and phenylalanine), a cysteine residue or methionine as sulfur-containing amino acids, and acid or nucleophilic amino acids like aspartate, glutamate or serine at the C-terminal end have been designed and tested towards their potency and selectivity to inhibit COX-2.[13,14]

Tripeptide inhibitor (H-Trp-Cys-Ser-OH) was identified as a potential lead for a new class of COX-2 inhibitors. The dissociation constant (K_D) for COX-2 with tripeptide peptide H-Trp-Cys-Ser-OH was determined to be 1.9×10^{-10} M using surface plasmon resonance. Another report describes the computer-aided, rational design of potent and selective small peptide inhibitors of COX-2. The identified tripeptides inhibited COX-2 with a predicted potency in the nanomolar range.[13,14] Among these examples, tripeptide inhibitor H-Trp-Tyr-Asp-OH showed an extraordinarily high affinity and selectivity towards COX-2 (K_D (COX-2) = 1.9×10^{-5} μM; K_D (COX-1) = 51.6 μM).[13] Moreover, the final docked position of tripeptide H-Trp-Tyr-Asp-OH with the COX-2 binding site revealed flexibility of the COX-2 binding pocket to accommodate substituents such as prosthetic groups at the N-terminal end of the tripeptides.[13]

These findings, along with the known three-dimensional structure of the COX-2 binding site, prompted us to design and synthesize various small peptides consisting of a hydrophobic aromatic amino acid (tyrosine, tryptophan or phenylalanine), a sulphur-containing amino acid (cysteine or methionine), and an acidic or nucleophilic amino acid (aspartate, glutamate or serine). In addition to this general peptide sequence, we have included a fluorobenzoyl residue at the N-terminal end to allow incorporation of the short-lived positron emitter ^{18}F into the peptide through acylation with bifunctional labeling agent [^{18}F]SFB.[23–26] In another set of peptides, we mimicked hydrophobic amino acids such as phenylalanine or tyrosine with fluorobenzoic acid to afford fluorobenzoylated dipeptides. A design scheme of fluorine-containing small peptides as novel selective COX-2 inhibitors is depicted in Figure 2.

All peptides were prepared following standard Fmoc-based solid phase peptide synthesis. Introduction of the fluorobenzoyl residue was accomplished according to our previously reported

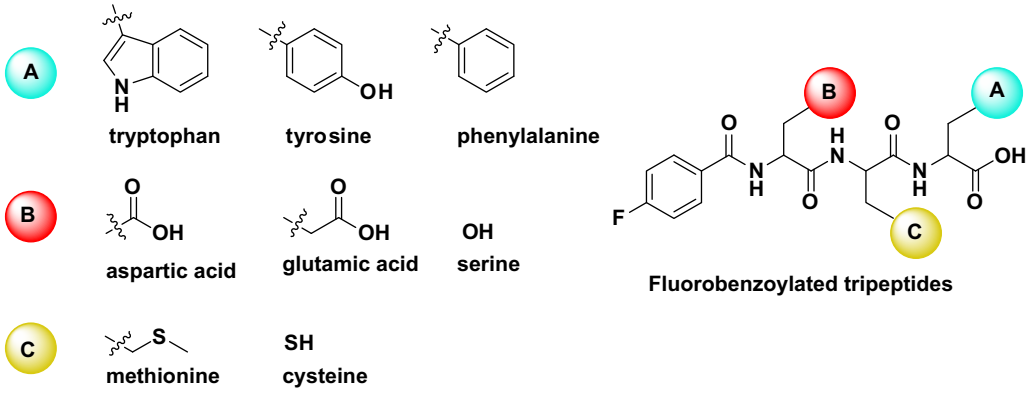

Figure 2. Design scheme of fluorine-containing small peptides as COX-2 inhibitors containing an aromatic amino acid residue (A), a sulfur-containing amino acid residue (B), and acidic amino acid (C) at the C-terminal end.

method.[24] After HPLC purification and lyophilisation, peptides were isolated as solids with purities greater than 98% as indicated by HPLC analysis. All peptides showed no decomposition after 3 months when appropriately stored in a refrigerator at −20 °C. Peptides **1–15** could be prepared in multi-milligram amounts to allow determination of their COX-2 inhibitory potency and selectivity in an in vitro COX binding assay.

All fluorobenzoylated peptides and previously reported high potent and COX-2 selective tripeptides H-Trp-Cys-Ser-OH and H-Trp-Tyr-Asp-OH were evaluated in a fluorescence-based COX assay to determine the different steric and electronic effects upon COX-1 and COX-2 inhibitory potency and selectivity. Potent and selective COX-2 inhibitor celecoxib was used as reference compound in the COX assay. The determined COX inhibitory data for celecoxib, H-Trp-Cys-Ser-OH, H-Trp-Tyr-Asp-OH, fluorobenzoylated tripeptides **1–10** and fluorobenzoylated dipeptides **11–15** are summarized in Table 1.

In our enzyme inhibitory assay, as expected, reference compound celecoxib showed high COX-2 inhibitory potency and selectivity with IC_{50} values of 0.04 μM for COX-2 and 15 μM for COX-1, which is consistent with our previously reported findings.[27]

Table 1
In vitro COX-1 and COX-2 enzyme inhibition data for celecoxib, di- and tripeptides

No.	Peptide	COX-1 IC_{50}[a] (μM)	COX-2 IC_{50}[a] (μM)
Celecoxib	—	15	0.04
	Trp-Cys-Ser	6	21 (K_D = 0.19 nM)[c]
	Trp-Tyr-Asp	n.i. (K_D = 51.6 μM)[d]	700 ($K_D = 1.9 \times 10^{-5}$ μM)[d]
1	FB-Trp-Met-Asp	n.i.b	450
2	FB-Trp-Met-Glu	n.i.	350
3	FB-Tyr-Met-Asp	n.i.	>1000
4	FB-Tyr-Met-Glu	n.i.	500
5	FB-Phe-Met-Asp	n.i.	450
6	FB-Phe-Met-Glu	n.i.	>1000
7	FB-Phe-Cys-Ser	27	13
8	FB-Trp-Cys-Ser	140	85
9	FB-Trp-Tyr-Asp	n.i.	n.i.
10	FB-Tyr-Trp-Ser	n.i.	180
11	FB-Cys-Ser	5	15
12	FB-Cys-Asp	15	14
13	FB-Tyr-Ser	n.i.b	140
14	FB-Trp-Ser	n.i.	200
15	FB-Tyr-Asp	n.i.	110

[a] Values listed are the means of two determinations.
[b] n.i.: no inhibition in the studied concentration range (10^{-9} to 10^{-3} M).
[c] Reported K_D value of peptide Trp-Cys-Ser for COX-2 determined by surface plasmon resonance spectroscopy. The same group reported an IC_{50} value of 15 nM determined by ELISA.[14]
[d] Reported K_D values determined using molecular docking study experiments.[13]

However, in our assay reference peptides H-Trp-Cys-Ser-OH and H-Trp-Tyr-Asp-OH displayed only very weak COX-2 inhibitory potency of 21 and 700 μM, respectively. This is in drastic contrast to previous reports describing both peptides as highly potent COX-2 inhibitors with K_D values in the subnanomolar range. Moreover, both peptides did also not show the reported high COX-2 selectivity profile. Instead, tripeptide H-Trp-Cys-Ser-OH displayed selectivity towards COX-1 (IC_{50} = 6 μM) rather than towards COX-2 (IC_{50} = 21 μM).

Compared to potent small molecule inhibitor celecoxib, all prepared fluorobenzoylated di- and tripeptides and reference peptides H-Trp-Cys-Ser-OH and H-Trp-Tyr-Asp-OH showed significantly weaker COX-2 inhibitory potency and selectivity. Among tripeptides, only cysteine-containing peptides **7** and **8** showed weak COX-2 inhibitory potency with IC_{50} values of 13 and 85 μM for COX-2, respectively, while also displaying low COX-2 selectivity profile (IC_{50} values of 27 and 140 μM for COX-1). This results in a COX-2 selectivity index (COX-2 SI) of 2.1 and 1.6, respectively, for peptides **7** and **8**. All other tripeptides displayed only very weak COX-2 inhibitory potency greater than 180 μM. Substitution of cysteine with other sulfur-containing amino acid methionine or aromatic amino acids tyrosine and tryptophan resulted in a significant reduction of COX-2 inhibitory potency. No inhibition of COX-1 was observed for tripeptides **1–6** and **8–10** within the studied concentration range. The trend of very low COX-2 inhibitory potency was also found within the series of fluorobenzoylated dipeptides **11–15** ranging from 14 to 200 μM. In this series of peptides, aromatic amino acids tryptophan, tyrosine or phenylalanine were replaced with fluorobenzoic acid to mimick tripeptides as originally reported in the literature. The highest COX-2 inhibitory potency was also found for cysteine-containing peptides (peptide **11** and **12**). Hence, the presence of a cysteine residue seems to be an important prerequisite for COX-2 binding. Moreover, in contrast to tripeptides **7** and **8**, cysteine-containing dipeptides showed different COX-2 selectivity profiles favoring COX-1 binding in the case of compound **11** and equal COX-1 binding for compound **12**.

The found weak COX-2 inhibitory potency and selectivity of fluorobenzoylated di- and tripetides **1–12** is in contrast to previously reported high affinity COX-2 binding peptides like tripeptides H-Trp-Cys-Ser-OH and H-Trp-Tyr-Asp-OH.[13,14] However, direct comparison of our results and results reported in the literature remains difficult since reported COX-binding data were obtained using surface Plasmon resonance and molecular modeling docking studies. This may explain the discrepancy between the COX-2 affinity and selectivity data reported in the literature and in this study.

Based on our data we conclude that the introduction of the fluorobenzoyl residue seems not to be responsible for the very weak

inhibitory potency and the very low COX-2 selectivity profile. This conclusion is supported by data obtained for fluorobenzoylated peptide **8** which showed a comparable micromolar IC_{50} value (85 μM) as reference peptide H-Trp-Cys-Ser-OH containing the same amino acid sequence. Moreover, it also seems to be feasible to extend this assumption to the other peptides studied in this work.

Binding of most potent and selective peptide **7** (FB-Phe-Cys-Ser-OH) within the active site of the COX-2 enzyme was further studied with molecular modeling docking experiments using the known crystal structure of the active binding site of murine COX-2.[28] The result is shown in Figure 3.

Peptide **7** binds in the binding pocket of COX-2 through the formation of various distinct hydrogen bonds and hydrophobic interactions with selected amino acid residues within the binding pocket. The binding free energy for docking peptide **7** into the COX-2 binding pocket was calculated to be $\Delta G = -10.36$ kcal/mol. The docking of peptide **7** into COX-1 binding pocket resulted in a calculated binding free energy $\Delta G = -8.26$ kcal/mol. This is in agreement with our experimental data on the COX-2 selectivity profile of peptide 7 (COX-2 SI = 2.1).

Peptide **7** makes several hydrogen bonds with amino acid residues of the binding pocket. In particular, the cysteine residue of peptide **7** is involved in H-bond formations as exemplified by OH groups of Ser353 and Tyr355. The measured distances of 2.47 and 2.72 Å, respectively, are in the range typically found for H-bonding interactions. An additional H-bond of the C-terminal end of peptide **7** with Ser530 (2.19 Å) further stabilizes the peptide in the binding pocket. The extensive formation of H-bonds involving the cysteine residue of peptide **7** offers a plausible explanation for the observed higher potency of cysteine-containing tripeptides such as **7** and **8** in comparison to other peptides of this series lacking a H-donor such as the sulfhydryl group in cysteine. Peptide **7** is also stabilized within the binding pocket through the formation of two distinct hydrophobic interactions involving the phenylalanine residue of peptide **7** which is sandwiched between Val349 and Leu531, and a possible hydrophobic interaction of the fluorobenzoyl residue **7** in with Tyr355.

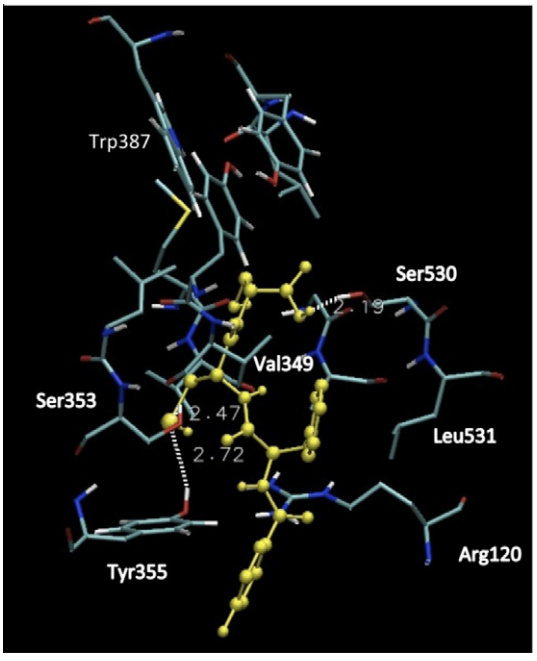

Figure 3. Docked position of peptide 7 with the active site of murine COX-2. Hydrogen atoms have been removed for more clarity except for amino acids of the binding pocket involved in H-bonds.

The found H-bonds between the cysteine residue with Ser353 and Tyr355, and the C-terminal end with Ser530, as well as the observed hydrophobic interactions of phenylalanine and fluorobenzoyl residue are in good agreement with the determined COX-2 inhibitory activity of peptide **7**. Moreover, these findings provide a reasonable explanation for the found higher inhibitory activity of other cysteine-containing compounds such as peptide **8**, **11**, and **12** in comparison with peptides lacking a cysteine residue.

3. Summary and conclusion

We have prepared and evaluated a series of small fluorobenzoylated di- and tripeptides as a novel class of COX-2 inhibitors. Most compounds studied showed only very week COX-2 inhibitory potency. Only cysteine-containing di- and tripeptides displayed IC_{50} values in the low micromolar range (5–85 μM). However, the determined COX-2 inhibitory potency of fluorobenzoylated peptides is much lower than the previously reported values for various tripeptides, which showed binding affinities in the subnanomolar range. Direct comparison of fluorobenzoylated peptide 8 with reference peptide H-Trp-Cys-Ser-OH suggests that introduction of the fluorobenzoyl group has no significant detrimental effect upon the COX-2 binding potency and selectivity. Instead, previously reported peptides seem to reflect too high potency and selectivity profiles as determined with surface plasmon resonance spectroscopy and molecular docking experiments.

The found low COX-2 inhibitory potency and selectivity of fluorobenzoylated peptides studied in this study do not warrant further exploration of their corresponding ^{18}F-labeled analogues as molecular probes for imaging COX-2 expression in vivo. Therefore, further research on the development of radiolabeled COX-2 inhibitors for molecular imaging purposed should be directed to alternative small molecules possessing common structural features of typical selective COX-2 inhibitors such as celecoxib.

4. Experimental

4.1. Peptide synthesis

Peptide syntheses were performed on an automated peptide synthesizer (Syro I, MultiSyn Tech, Germany). All chemicals were reagent grade and used without further purification. Fmoc amino acid derivatives used in the peptide synthesis were purchased from MultiSyn Tech. Mass spectra were obtained on a Quattro/LC mass spectrometer (MICROMASS) by electrospray ionization. Reference peptides H-Trp-Cys-Ser-OH and H-Trp-Tyr-Asp-OH were prepared according to literature procedures.[13,14]

Peptides were prepared on alkoxybenzyl alcohol resins with an initial load of 0.6 mmol/g. Syntheses were performed on a 30–60 μmol scale. The Fmoc protecting group was removed with 20% piperidine in DMF for 15 min. The carboxyl group of the incoming amino acid or 4-fluorobenzoic acid was activated with HBTU and HOBt. Fmoc-amino acid or 4-fluorobenzoic acid (4.0 equiv), HBTU (3.6 equiv), HOBt (4.0 equiv), and DIPEA (7.2 equiv) were dissolved in DMF or NMP, respectively, and added to the resin. The coupling time was 1 h. Peptides were deprotected and cleaved from solid support with trifluoroacetic acid/dithiothreitol/water/triisopropyl-silane (88:5:5:2) for 3 h. The resin was filtered off and the crude peptide was precipitated by adding cold diethyl ether and washed with diethyl ether. The residual ether was removed by evaporation.

Pure peptides were obtained as white powders after purification with semi-preparative HPLC and subsequent lyophilization. Semi-preparative HPLC was performed using a HP 1050 system

with a Zorbax 300 SB-C18 column (9.4 × 250 mm, 5 μm). 0.1% of TFA in CH_3CN (A) and 0.1% of TFA in water (B) was used as the eluents at a flow rate of 2 mL/min and UV detection at 220 nm. The following gradient was used: 0–5 min 10% A, 10 min 10% A, 20 min 30% eluent A, 30 min 50% eluent A.

Analytical HPLC was performed using a HP 1100 system equipped with a Kromasil-C18 column (250 × 4.6 mm, 5 μm). Gradient elution was carried out at a flow rate of 1 mL/min. UV signals were detected at 220 nm.

Solvent A: 0.1% of TFA in water; solvent B: 0.1% of TFA in CH_3CN.

Method A: 0 min 40% B, 25 min 65% B, 25 min 100% B, 30 min 100% B.

Method B: 0 min 30% B, 25 min 55% B, 25 min 100% B, 30 min 100% B.

Method C: 0 min 25% B, 25 min 50% B, 25 min 100% B, 30 min 100% B.

4.1.1. FB-Trp-Met-Asp (1)

Yield: 61%. HPLC-analysis, method A, t_R = 9.0 min). MW $C_{27}H_{29}FN_4O_7S$ calculated 572.61, found LR-MS (ESI, negative): 571.17 $[M-H]^-$.

4.1.2. FB-Trp-Met-Glu (2)

Yield: 52%. HPLC-analysis, method A t_R = 9.1 min). MW $C_{28}H_{31}FN_4O_7S$ calculated 586.63, found LR-MS (ESI, negative): 585.35 $[M-H]^-$.

4.1.3. FB-Tyr-Met-Asp (3)

Yield: 55%. HPLC-analysis, method A, t_R = 7.5 min). MW $C_{25}H_{28}FN_3O_6S$ calculated 549.57, found LR-MS (ESI, negative): 548.22 $[M-H]^-$.

4.1.4. FB-Tyr-Met-Glu (4)

Yield: 43%. HPLC-analysis, method A, t_R = 7.4 min). MW $C_{26}H_{30}FN_3O_8S$ calculated 563.60, found LR-MS (ESI, positive): 564.17 $[M+H]^+$, 586.17 $[M+Na]^+$.

4.1.5. FB-Phe-Met-Asp (5)

Yield: 59%. HPLC-analysis, method A, t_R = 11.3 min). MW $C_{25}H_{28}FN_3O_7S$ calculated 533.57, found LR-MS (ESI, positive): 534.27 $[M+H]^+$, 556.18 $[M+Na]^+$.

4.1.6. FB-Phe-Met-Glu (6)

Yield: 55%. HPLC-analysis, method A, t_R = 9.3 min). MW $C_{26}H_{30}FN_3O_7S$ calculated 547.60, found LR-MS (ESI, positive): 548.25 $[M+H]^+$, 570.25 $[M+Na]^+$.

4.1.7. FB-Phe-Cys-Ser (7)

Yield: 34%. HPLC-analysis, method B, t_R = 13.7 min). MW $C_{22}H_{24}FN_3O_6S$ calculated 477.51, found LR-MS (ESI, negative): 476.30 $[M-H]^-$.

4.1.8. FB-Trp-Cys-Ser (8)

Yield: 41%. HPLC-analysis, method A, t_R = 9.6 min). MW $C_{24}H_{25}FN_4O_6S$ calculated 516.54, found LR-MS (ESI, negative): 515.30 $[M-H]^-$.

4.1.9. FB-Trp-Tyr-Asp (9)

Yield: 66%. HPLC-analysis, method A, t_R = 7.5 min). MW $C_{31}H_{29}FN_4O_8$ calculated 604.58, found LR-MS (ESI, positive): 605.20 $[M+H]^+$, 627.13 $[M+Na]^+$.

4.1.10. FB-Tyr-Trp-Ser (10)

Yield: 63%. HPLC-analysis, method B, t_R = 12.5 min). MW $C_{30}H_{29}FN_4O_7$ calculated 576.57, found LR-MS (ESI, positive): 577.06 $[M+H]^+$, 599.08 $[M+Na]^+$.

4.1.11. FB-Cys-Ser (11)

Yield: 55%. HPLC-analysis, method C, t_R = 8.6 min). MW $C_{13}H_{15}FN_2O_5S$ calculated 330.33, found LR-MS (ESI, negative): 328.95 $[M-H]^-$.

4.1.12. FB-Cys-Asp (12)

Yield: 58%. HPLC-analysis method C, t_R = 8.3 min). MW $C_{14}H_{15}FN_2O_6S$ calculated 358.34, found LR-MS (ESI, negative): 356.90 $[M-H]^-$.

4.1.13. FB-Tyr-Ser (13)

Yield: 68%. HPLC-analysis, method C, t_R = 7.9 min). MW $C_{19}H_{19}FN_2O_6$ calculated 390.36, found LR-MS (ESI, negative): 389.05 $[M-H]^-$.

4.1.14. FB-Trp-Ser (14)

Yield: 63%. HPLC-analysis, method B, t_R = 11.06 min). MW $C_{21}H_{20}FN_3O_5$ calculated 413.40, found LR-MS (ESI, negative): 412.05 $[M-H]^-$.

4.1.15. FB-Tyr-Asp (15)

Yield: 56%. HPLC-analysis, method C, t_R = 8.7 min). MW $C_{20}H_{19}FN_2O_7$ calculated 418.37, found LR-MS (ESI, positive): 419.15 $[M+H]^+$.

4.2. In vitro cyclooxygenase (COX) inhibition assay

The ability of peptides **1–15** and celecoxib to inhibit ovine COX-1 and recombinant human COX-2 was determined using a COX fluorescence inhibitor assay (catalog number 700100, Cayman Chemical, Ann Arbor, MI, USA) according to the manufacturer's assay protocol. Peptides 1-15 were assayed in concentrations ranging from 10^{-9} to 10^{-3} M. PRISM5 software was used for the calculation of IC_{50} values.

4.3. Molecular modeling docking experiments

For the docking studies we used only chain A of 1PXX. Docking of peptide **7** was performed using AutoDock 4. The following protocol was used for the docking studies: application of the Lamarckian genetic algorithm with 150 individuals in the population; a maximum of 25 × 106 energy evaluations; a mutation rate of 0.02; a crossover rate of 0.80, and the elitism value of 1. For the local search, pseudo-Solis and Wets algorism was applied using a maximum of 300 iterations per local search. The probability of performing local search on individuals in the populations was set to 0.6. The maximum number of consecutive successes or failures before doubling or halving the local search step was set to 4. 100 independent docking runs were performed. Results differing by 2.0 Å in positional root-mean-square deviation were clustered.

Acknowledgments

The authors would like to thank the Dianne and Irving Kipnes Foundation and the Canadian Institute for Health Research (CIHR) for supporting this work.

References and notes

1. Kurumbail, R. G.; Kiefer, J. R.; Marnett, L. J. *Curr. Opin. Struct. Biol.* **2001**, *11*, 752.
2. Marnett, L. J. *Curr. Opin. Chem. Biol.* **2000**, *4*, 545.
3. Fitzpatrick, F. A. *Curr. Pharm. Des.* **2004**, *10*, 577.
4. Marnett, L. J.; Rowlinson, S. W.; Goodwin, D. C.; Kalgutkar, A. S.; Lanzo, C. A. *J. Biol. Chem.* **1999**, *274*, 22903.
5. Smith, W. L.; Garavito, R. M.; DeWitt, D. L. *J. Biol. Chem.* **1996**, *271*, 33157.
6. Herschman, H. R. *Biochim. Biophys. Acta* **1996**, *1299*, 125.
7. Ritter, J. M.; Harding, I.; Warren, J. B. *Trends Pharmacol. Sci.* **2009**, *10*, 503.
8. Brophy, J. M. *Expert Opin. Drug. Saf.* **2005**, *6*, 1005.

9. Singh, P.; Mittal, A. *Mini-Rev. Med. Chem.* **2008**, *8*, 73.
10. Jawabrah Al-Hourani, B.; Sharma, S. K.; Suresh, M.; Wuest, F. *Expert Opin. Ther. Pat.* **2011**, *21*, 1339.
11. Jachak, S. M. *Curr. Med. Chem.* **2006**, *13*, 659.
12. Rao, P.; Knaus, E. E. *J. Pharm. Pharm. Sci.* **2008**, *11*, 81s.
13. Rajakrishnan, V.; Manoj, V. R.; Subba Rao, G. *J. Biomol. Struct. Dyn.* **2008**, *25*, 535.
14. Somvanshi, R. K.; Kumar, A.; Kant, S.; Gupta, D.; Singh, S. B.; Das, U.; Srinivasan, A.; Singh, T. P.; Dey, S. *Biochem. Biophys. Res. Commun.* **2007**, *361*, 37.
15. Kothekar, V.; Sahi, S. *J. Mol. Struct. Theochem.* **2002**, *577*, 107.
16. Kapoor, V.; Singh, A. K.; Dey, S.; Sharma, S. C.; Das, S. N. *J. Cancer Res. Clin. Oncol.* **2010**, *136*, 1795.
17. Wuest, F.; Höhne, A.; Metz, P. *Org. Biomol. Chem.* **2005**, *3*, 503.
18. Wuest, F.; Kniess, T.; Bergmann, R.; Pietzsch, J. *Bioorg. Med. Chem.* **2008**, *16*, 7662.
19. de Vries, E. F.; van Waarde, A.; Buursma, A. R.; Vaalburg, W. *J. Nucl. Med.* **2003**, *44*, 1700.
20. McCarthy, T. J.; Sheriff, A. U.; Graneto, M. J.; Talley, J. J.; Welch, M. J. *J. Nucl. Med.* **2002**, *43*, 117.
21. Prabhakaran, J.; Underwood, M. D.; Parsey, R. V.; Arango, V.; Majo, V. J.; Simpson, N. R.; Van Heertum, R.; Mann, J. J.; Kumar, J. S. *Bioorg. Med. Chem.* **2007**, *15*, 1802.
22. Kuhnast, B.; Dolle, F. *Curr. Radiopharm.* **2010**, *3*, 174.
23. Mäding, P.; Füchtner, F.; Wuest, F. *Appl. Radiat. Isotop.* **2005**, *63*, 329.
24. Hultsch, C.; Berndt, M.; Bergmann, R.; Wuest, F. *Appl. Radiat. Isotop.* **2007**, *65*, 818.
25. Wuest, F.; Vogler, L.; Berndt, M.; Pietzsch, J. *Amino Acids* **2009**, *36*, 283.
26. Richter, S.; Bergmann, R.; Pietzsch, J.; Ramenda, T.; Steinbach, J.; Wuest, F. *Biopolymers* **2009**, *92*, 479.
27. Jawabrah Al-Hourani, B.; Sharma, S. K.; Mane, J. Y.; Tuszynski, J.; Baracos, V.; Kniess, T.; Suresh, M.; Pietzsch, J.; Wuest, F. *Bioorg. Med. Chem. Lett.* **2011**, *21*, 1818.
28. The crystal structure of COX-2 inhibitor diclofenac bound to murine COX-2 enzyme was obtained from the RCSB Protein Data Bank (PDB identifier 1PXX).